Modular Access to Structurally Switchable Three-Dimensional DNA Assemblies

Faisal A. Aldaye and Hanadi F. Sleiman*

Department of Chemistry, McGill University, 801 Sherbrooke St. West, Montreal, QC, H3A 2K6, Canada

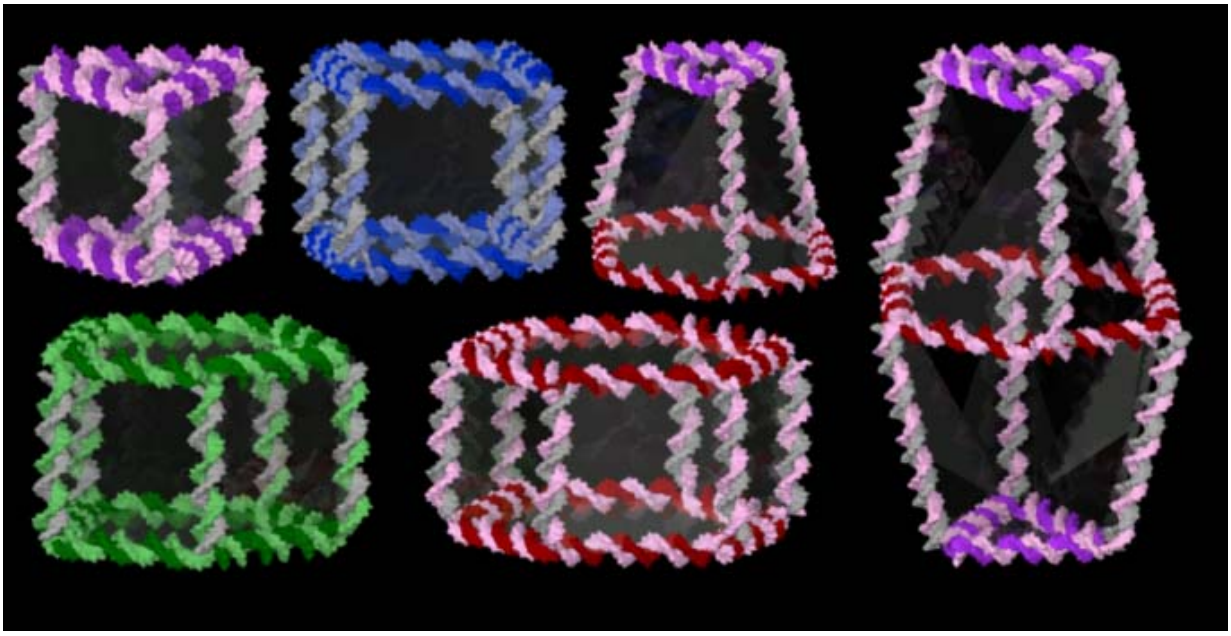

In this contribution we describe a facile method to access a large number of three-dimensional discrete DNA assemblies. The approach involves the use of single-stranded and cyclic DNA building blocks, of predefined geometry, as the faces or sides of the objects to be constructed. Any target three-dimensional discrete object that could be retrosynthetically broken down into a combination of our discrete shapes, could in principle be easily accessed using this method. Using triangle **3**, square **4**, pentagon **5** and hexamer **6**, we constructed triangular, cubic, pentameric and hexameric prisms, as well as the more complex heteroprism **HP** and biprism **BP** assemblies shown above. The use of single-stranded DNA building blocks inherently allows for dynamic character and addressability. Using a series of rigidifying and eraser strands, we generated a triangular prism capable of structural oscillation between three predefined lengths (see right). The easy access to a large number of complex three-dimensional discrete DNA objects, that are also dynamic in response to external stimuli, promises to expand the applications of 3D DNA construction in many areas of nanoscience.

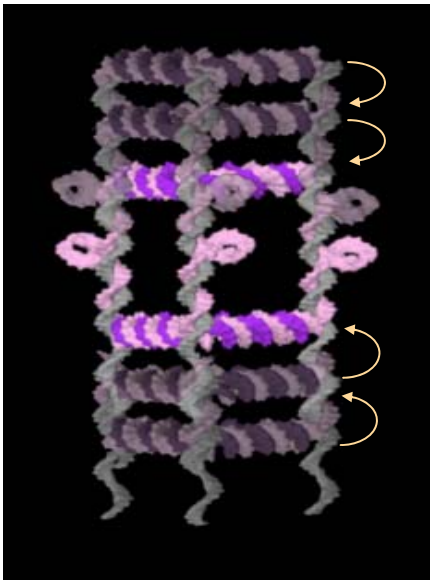

Contents

I. General

Acetic acid, boric acid, cyanogen bromide (5M in acetonitrile), EDTA, formamide, 4-morpholineethanesulfonic acid (MES), $MgCl_2$, StainsAll®, and tris(hydroxymethyl)-aminomethane (Tris) were used as purchased from Aldrich. 1000Å base derivatized LCAA-CPG solid support with a loading density of 32 μmol/g for general DNA synthesis, 2000Å phosphate-CPG with a loading density of 15 μmol/g, 5-ethylthiotetrazole, and reagents for automated DNA synthesis were used as purchased from ChemGenes. Sephadex G-25 (super fine DNA grade), Mung Bean Nuclease (MBN, source: Mung Bean Sprouts), and Exonuclease VII (ExoVII, source: recombinant) were used as purchased from Amersham Biosciences. Microcon® size-exclusion centrifugal filter devices were purchased from Millipore. 5-carboxy-X-rhodamine (ROX) and 4'-(4-nitrophenyldiazo)-2'-methoxy-5'-methoxyazobenzene (BHQ-2) end-labeled DNA strands were used as purchased from Sigma-Genosys (HPLC purified).

II. Instrumentation

Standard automated oligonucleotide solid-phase synthesis was performed on a Perspective Biosystems Expedite 8900 DNA synthesizer. UV-vis measurements were conducted on a Varian Cary 300 biospectrophotometer. Gel electrophoresis experiments were carried out on an acrylamide 20 X 20 cm vertical Hoefer 600 electrophoresis unit. Electroelution was performed using a Centrilutor® electroeluter from Millipore. Matrix assisted laser desorption time-of-flight (MALDI-TOF) spectra were obtained using a KOMPACT MALDI III mass spectrometer. Fluorescence experiments were conducted using a Photon Technology International TimeMaster spectrofluorimeter (model C-720F).

III. Synthesis of triangle 3, square 4, pentamer 5 and hexamer 6

The set of single-stranded and cyclic DNA building blocks to be synthesized are triangle **3**, square **4**, pentamer **5** and hexamer **6** (Scheme S1 top panel). The approach involves synthesis of a single continuous DNA strand embedded with the appropriate number of rigid organic vertex **1** molecules (i.e. three for triangle **3**, four for square **4**, five for pentamer **5** and six for hexamer **6**), its cyclization using the respective template strand **T**, and its subsequent chemical ligation to afford the respective cyclic DNA building block. This is exemplified in Scheme S1 (bottom panel) for triangle **3**.

Scheme 1

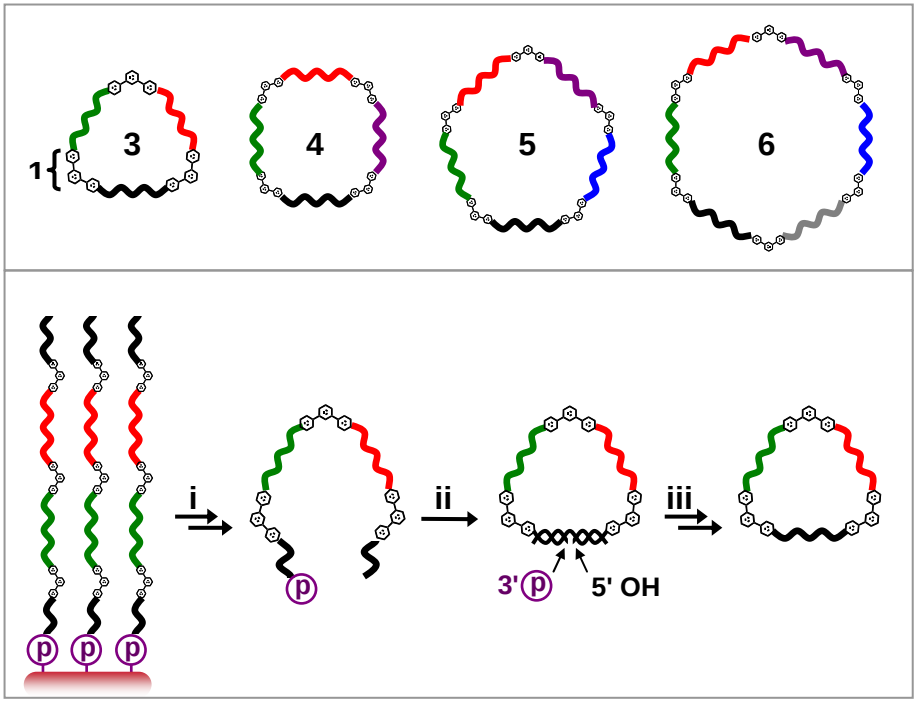

(Top panel) Single-stranded and cyclic DNA building blocks triangle **3**, square **4**, pentagon **5** and hexamer **6**. (Bottom panel) DNA of the appropriate length, sequence, and number of vertex **1** molecules is (i) synthesized on phosphate-CPG to afford the *linear analogue* of triangle **3**. (ii) These strands are then cyclized using a complementary template strand, and (iii) are chemically ligated to yield the final single-stranded and cyclic triangle **3**, following purification from denaturing polyacrylamide gel electrophoresis.

Initial work was directed towards the synthesis of each respective continuous strand (i.e. linear analogous of **3**, **4**, **5** and **6**) (Scheme S2). Synthesis was conducted on phosphate-CPG with a loading density of 15 µmol/g and a pore size of 2000Å. Incorporation of a phosphate into the 3' position of each strand facilitates its chemical ligation. Standard DNA synthesis was conducted using typical oligonucleotide synthetic protocols, while couplings of vertex **1** using a trityl protected amidite derivative **2** were performed with extended coupling and deprotection times of 15 and 2 minutes. For example, triangle **3** is constructed by synthesizing thirty bases of the appropriate sequence that are embedded with three units of vertex **1**, using **2**, after positions 5, 15, and 25 (Scheme 1 bottom panel). Synthesis of vertex **2**, the trityl protected amidite derivative of **1**, has been previously reported.[S1]

Scheme S2

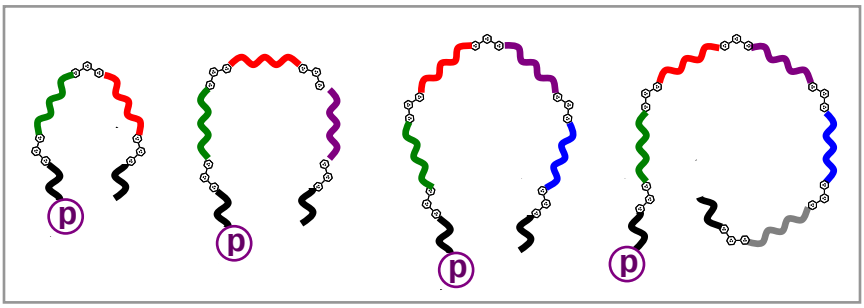

Cleavage and deprotection from the solid support was carried out in a concentrated solution of ammonium hydroxide (55°C, 12 hours). The crude syntheses were purified on 24% polyacrylamide 7 molar urea gels (up to 20 AU_{260} of crude DNA per gel) using 0.09M Tris-borate-EDTA buffer (pH 8.3). Following electrophoresis, the plates were wrapped with plastic wrap (Saran Wrap®), placed on a fluorescent TLC plate, and illuminated with a UV lamp (254 nm). The bands corresponding to the desired products were excised, and the gel pieces were crushed and incubated in 3 mL of sterile water (37ºC, 16 hours). The tubes were then vortexed and centrifuged, and the supernatants were lyophilized and desalted using Sephadex G-25 size exclusion column chromatography. Quantification was carried

out by UV-vis analysis using Beer's law ($A_{total} = A_{vertex} + A_{DNA}$), in which the extinction coefficient of each unit of vertex **1** at 260 nm was calculated to be 2.30 X 10^5 L mol^{-1} cm^{-1}.

Matrix assisted laser desorption ionization time-of-flight (MALDI-TOF) mass spectrometry was used to characterize the linear, uncyclized, analogous of triangle **3**, square **4**, pentamer **5** and hexamer **6** (along with the respective template strands **T** used to cyclize them). MALDI-TOF MS was performed using a co-matrix composed of 6-aza-2-thiothymine and fucose, and the additive spermine. The matrix was prepared according to a procedure reported by Distler *et al.*[S2] The theoretically calculated molecular masses (MM), experimentally obtained MM, and the respective sequence of each building block is summarized in Table S1.

Table S1. Sequences and MALDI-TOF MS obtained molecular masses of the *linear analogue* of the building block and of their respective template strands.

	Sequence (5' → 3')	Cal / Exp (g/mol)
3a	TTGTG-**1**-TTATTGGTCA-**1**-TTAGGTTGAA-**1**-CCGAT-**Phosphate**	1,0335.9 / 1,0360.0 [M + Na^+]
3b	TGTCA-**1**-GAGTATGAGC-**1**-AGCCAACCAA-**1**-GGTGA-**Phosphate**	1,0351.0 / 1,3449.0
4a	TTGTG-**1**-TTATTGGTCA-**1**-TTAGGTTGAA-**1**-AGGTTTGCTG-**1**-CCGAT-**Phosphate**	13,795.35 / 13,831.6 [M + K^+]
4b	TGTCA-**1**-AGCCAGATTT-**1**-GAGTATGAGC-**1**-AGCCAACCAA-**1**-GGTGA-**Phosphate**	15,707.7 / 15,707.0
5a	TTGTG-**1**-TTATTGGTCA-**1**-TTAGGTTGAA-**1**-AGGTTTGCTG-**1**-GGAACTCTTG-**1**-CCGAT-**Phosphate**	17,224.7 / 17,249.0 [M + Na^+]
5b	TGTCA-**1**-AGGTGATGTC-**1**-AGCCAGATTT-**1**-GAGTATGAGC-**1**-AGCCAACCAA-1-GGTGA-**Phosphate**	17,233.8 / 17,258.7 [M + Na^+]
6a	TTGTG-**1**-TTATTGGTCA-**1**-TTAGGTTGAA-**1**-AGGTTTGCTG-**1**-GGAACTCTTG-**1**-AAGGTAGGAA-**1**-CCGAT-**Phosphate**	21,049.39 / 21,086.3 [M + K^+]
6b	TGTCA-**1**-CGGGCGTCCA-**1**-AGGTGATGTC-**1**-AGCCAGATTT-**1**-GAGTATGAGC-**1**-AGCCAACCAA-**1**-GGTGA-**Phosphate**	20,649.1 / 20,649.9
Ta	CACAAATCGG	3,110.0 / 3,108.9
Tb	TGACATCACC	3,060.9 / 3,061.4

The clean isolation of the linear analogues of triangle **3**, square **4**, pentamer **5** and hexamer **6** was demonstrated using a 24% polyacrylamide gel (Figure S1). Gels are visualized following staining in a

solution of StainsAll® for two hours (12.5 mg StainsAll® in 125 mL of distilled water and 125 mL of formamide).

With the single-stranded linear analogous in hand, work was then directed towards their cyclization and subsequent chemical ligation. Hybridizations were conducted by combining 2.2 X 10^{-10} moles of each building block with 2.2 X 10^{-10} moles of the cyclization template strand, in 10 µL of MES buffer (250 mM MES and 20 mM $MgCl_2$, pH of 7.6) at 0ºC for 10 minutes. The ligation of these assemblies using cyanogen bromide was then conducted according to a procedure reported by Carreiro *et al.*[S3] In order to confirm the potential and efficiency of this approach for ligating a 5' hydroxyl strand to a 3' phosphate strand, studies were performed on a control system made up of three simple linear strands (Figure S2a). 10 µL of cyanogen bromide

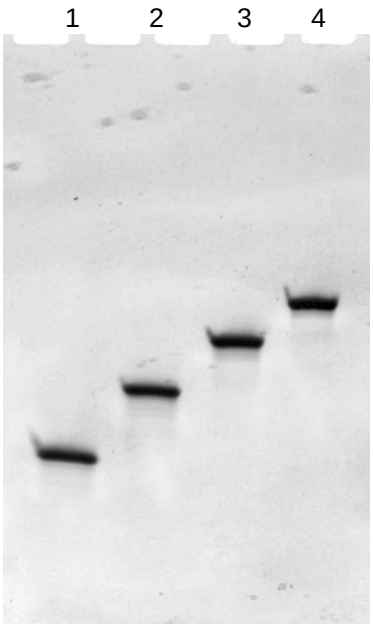

Figure S1. 24% denaturing polyacrylamide gel characterization of the purified *linear analogues* of triangle **3**, square **4**, pentagon **5** and hexagon **6** (lanes 1, 2, 3 and 4, respectively).

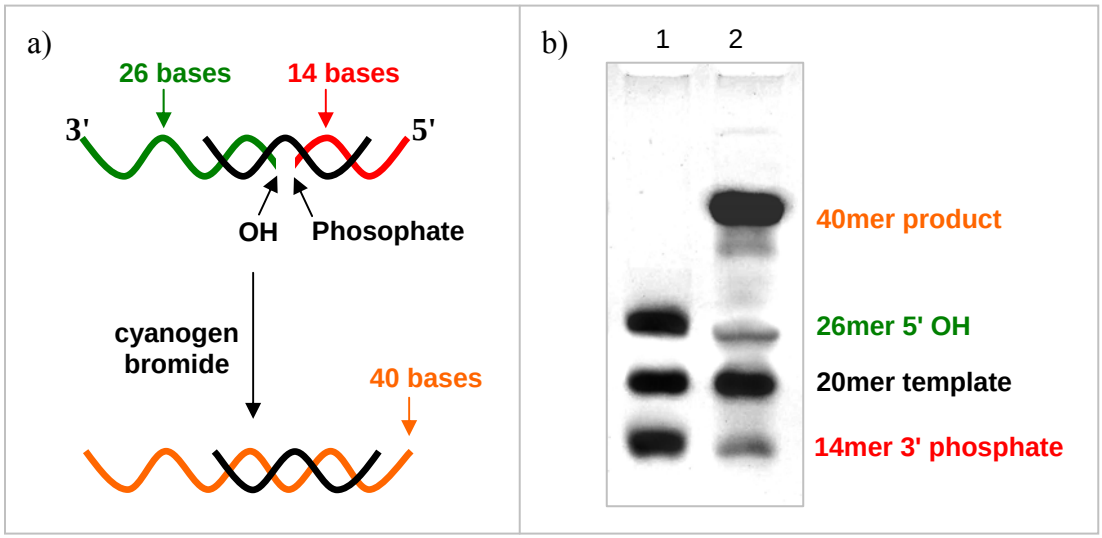

Figure S2. (a) When a 26mer 5'-OH and a 14mer 3'-phosphate strand, templated by a 20mer strand, are chemically ligated using cyanogen bromide a 40mer strand of DNA is generated. (b) This is indeed confirmed using a 24% denaturing polyacrylamide gel (lane 1 pre-ligation, lane 2 post-ligation).

(5 M in acetonitrile) was added to the DNA strands to be ligated in 30 μL of MES buffer, and was left incubating at 0ºC for 15 minutes. The DNA was recovered following addition of 350 μL of 2% $LiClO_4$ (in acetone), precipitation on dry ice for 15 minutes, centrifugation at 13,000 rpm for 3 minutes, removal of the supernatant (i.e. decant), and lyophilization of the residual solution. As seen by the 24% denaturing polyacrylamide gel in Figure S2b, the use of cyanogen bromide to chemically ligate a 5' hydroxyl to a 3' phosphate proceeds with an overall efficiency that is greater than 80%.

The hybridized cyclic triangular, square, pentameric and hexameric building blocks were thus ligated following the addition of 10 μL of cyanogen bromide (in a total volume of 30 μL of MES buffer) and were left incubating at 0ºC for 15 minutes. Analysis of the crude mixtures generated following ligation of hybridized cyclic **3**, **4**, **5** or **6** revealed the formation of a single other major product (Figure S3).

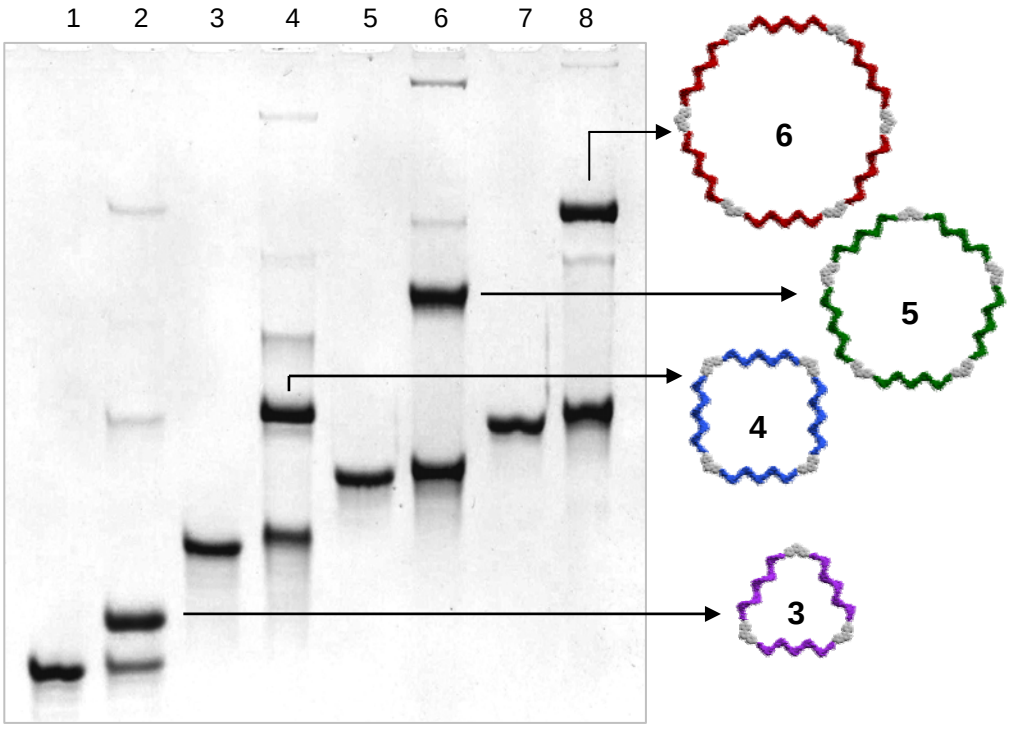

Figure S3. Upon ligation of the linear analogues of **3**, **4**, **5** and **6** (lanes 1, 3, 5 and 7, respectively) a single other product is generated assigned to triangle **3**, square **4**, pentamer **5** and hexamer **6** (lanes 2, 4, 6 and 8, respectively).

In all cases, this product is retarded in electrophoretic mobility, when compared to the unligated linear analogues, and is assigned to the respective cyclic triangle **3**, square **4**, pentamer **5**, and hexamer **6**.

To confirm the cyclic and single-stranded nature of **3**, **4**, **5** and **6**, enzymatic digestions assays using ExoVII were conducted. ExoVII is selective for the digestion of single-stranded DNA that is linear, and will *not* be effective on cyclic DNA even if it is single-stranded. To ensure that the enzyme is active on DNA containing the rigid organic vertex **1**, and to determine the optimal conditions under which single-stranded and linear DNA is digested, the linear analogue of triangle **3** was subjected to digestions using varying amounts of ExoVII. Digestions were performed at 37ºC for a period of 22 minutes. In all these cases, 1.2 X 10^{-10} moles of DNA in 10 μL of TAEmg buffer (40 mM Tris, 20 mM acetic acid, 2 mM EDTA, 12.5 mM $MgCl_2$) was subjected to 0.5, 1, 3 and 5 units of ExoVII. As seen in Figure S4, addition of 5 units of the enzyme results in complete degradation of the single-stranded species. The crude mixtures resulting from the ligation of each cyclized building block were thus subjected to this same enzymatic digestion condition (i.e. 5 units of ExoVII, at 37ºC for 22 minutes). In all cases, the linear starting material was completely digested, while the bands assigned to the cyclic products were unaffected (Figure S5),

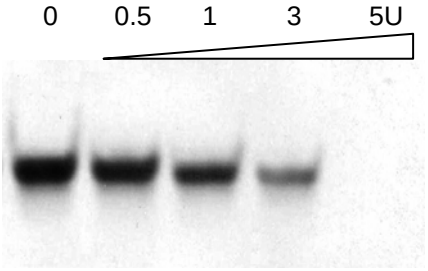

Figure S4. The use of 5 units of ExoVII (37ºC, 22 minutes) results in complete degradation of single-stranded DNA.

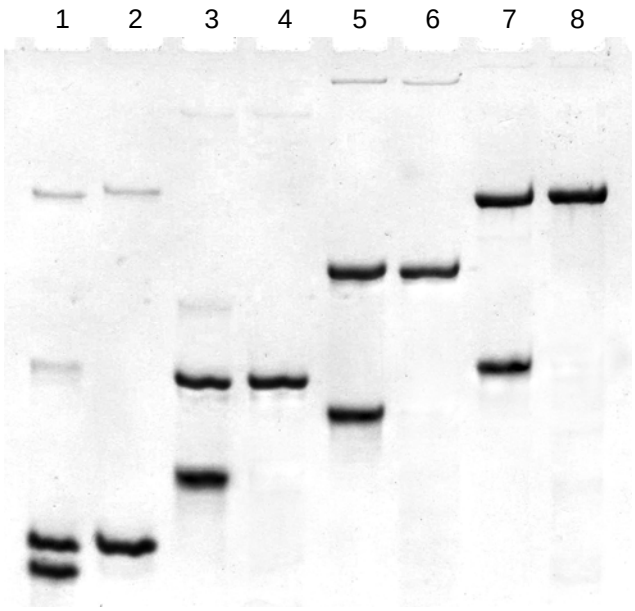

Figure S5. ExoVII digestion of the crude mixture resulting from the ligation of **3**, **4**, **5** and **6** (lanes 1, 3, 5 and 7, respectively) confirms the band assignment of cyclic triangle **3**, square **4**, pentagon **5** and hexagon **6** (lanes 2, 4, 6 and 8, respectively).

confirming our initial assignments. Triangle **3**, square **4**, pentagon **5** and hexagon **6** were then further purified following direct electroelution from the gels using a Centrilutor® electroeluter.[S1] MALDI-TOF MS analysis also confirm our band assignements (Table S2).

Table S2. Calculated and MALDI-TOF MS obtained molecular masses of cyclic single-stranded triangle **3**, square **4**, pentamer **5** and hexamer **6**.

3a	10,317.0 / 10,310.0	**3b**	10,333.0 / 10,350.1 [M + Na^+]
4a	13,777.4 / 13,794.5 [M + Na^+]	**4b**	15,689.7 / 15,694.0
5a	17,206.7 / 17,232.1 [M + Na^+]	**5b**	17,215.8 / 17,217.2 [M + K^+]
6a	21,031.4 / 21,033.7	**6b**	20,631.1 / 20,636.7

IV. Triangular P3, square P4, pentameric P5 and hexameric prism P6

Triangular prism **P3** is generated following the addition of two units of triangle **3**, **3a** and **3b**, to three linking strands (**LS 1-3**) that are subsequently made double-stranded using complementary rigidifying strands (**RS1**). Scheme S3 summarizes the general assembly concept used in constructing this discrete DNA object. Hybridizations are typically conducted by combining all the DNA strands in the correct molar ratio (3 X 10^{-10} moles of the final assembly) in 10 µL of TAEmg buffer, and by incubating the system at 0ºC for 15 minutes. The quantitative assembly of prism **P3**, as well as all the possible intermediates leading up to its construction, are analyzed using 10% native polyacrylamide gel electrophoresis (10 mA, 4°C, 17 hours) (Figure 1a, manuscript).

Scheme S3

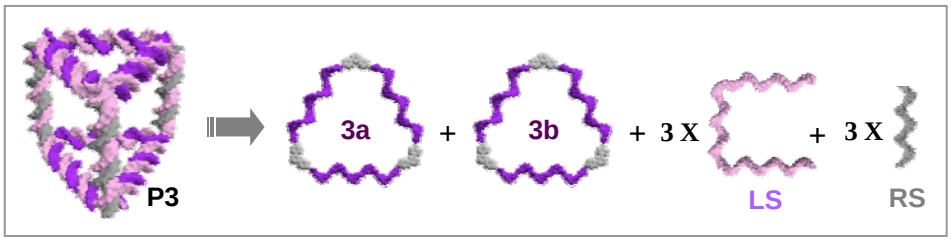

A series of enzymatic digestion assays were conducted in order to confirm the connectivity within prism **P3**. The enzyme Mung bean nuclease (MBN) is selective for the digestion of single-stranded DNA over that of double-stranded DNA by a factor of 30,000:1.[S4] This enzyme possesses both exo- and endonuclease activity, and will thus digest any portion of DNA within the assembly that is single-stranded. The exonuclease ExoVII is also selective for the digestion of single-stranded DNA, but will only digest open DNA (i.e. uncylized) and is thus *only* capable of digesting single-stranded DNA within an assembly that is uncyclized. Conditions for the digestion of "our" DNA have been determined for MBN[S1] and for ExoVII (see Section III). The single-stranded analogue of prism **P3,** made from two units of triangle **3**, three linking strands, and *none* of the rigidifying strands, was digested by MBN but not by ExoVII (Figure 1b lanes 4-6, manuscript). This is in agreement with the fact that it contains single-stranded DNA that is not end-exposed for access by ExoVII. Furthermore, the intermediate assembly generated form a single unit of triangle **3** and three single-stranded linking strands was degraded by both MBN and ExoVII (Figure 1b lanes 7-9, manuscript). Importantly, both enzymes were incapable of digesting any part of prism **P3** (Figure 1b lanes 1-3, manuscript), indicating that all the DNA stands within this assembly are double-stranded and cyclized and confirming the assigned connectivity within **P3**.

Self-assembly and generation of triangular prism **P3** was also monitored in real-time using fluorescence resonance energy transfer (FRET) studies. A single linker strand (**LS1**) was dually end-labeled with the fluorophore and quencher ROX / BHQ-2, and was used to monitor the sequential self-assembly dynamics leading to the generation of prism **P3**. The dually labeled probes were quantified and used as supplied from Sigma-Genosys. Given that the fluorophore ROX has a quantum yield Φ of 0.7, and using the respective emission and absorption spectra of ROX and BHQ-2 (Figure S6), an overlap integral $J(\lambda)$ of 3.89289×10^{-13} $M^{-1}cm^3$ and a Förster distance R_o of 5.89 nm is calculated.[S5] In

all these experiments, measurements were performed on 2 X 10^{-10} moles of the final capsule, and the probe, in a total volume of 75 µL of TAEmg buffer at room temperature. Samples were excited at 570 nm and monitored at 602 nm. Measurements conducted on just the double-stranded probe were performed in order to determine the fluorescence magnitude of totally unquenched ROX, which can only be done since the length of a double-stranded 30mer is more than twice the Förster distance (Figure S7a). Assembly of one unit of triangle **3** hybridized to all three linking strands **P3-3** emits at 24% of the totally unquenched species, which using the calculated Förster distance of 5.89 nm translates into a distance of 4.9 nm. Upon addition of the second unit of triangle **3** to generate the single stranded analogue of P3 (**P3ss**), i.e. addition of triangle **3b** to an assembly of triangle **3a** and three single-stranded linker strands, fluorescence with a magnitude of 15% the unquenched standard is observed. This translates into a distance of 4.4 nm, and reveals an even more dynamic character within the fully cyclized single-stranded analogue of prism **P3**. The fully hybridized triangular prism **P3** fluoresces at 40% the unquenched probe, indicating that the distance between the fluorophore and the quencher within prism **P3** (i.e. the prism's length) is 5.2 nm. This is in approximate agreement with the expected value for a 10 base long prism.

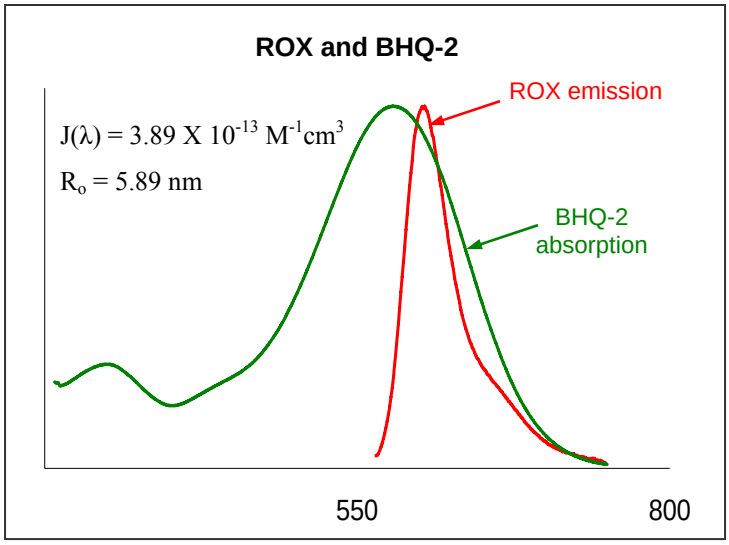

Figure S6. An overlap integral J(λ) of 3.89289 X 10^{-13} $M^{-1}cm^3$ and Förster distance R_o of 5.89 nm was calculated for the donor acceptor pair ROX / BHQ-2, using their respective fluorescence and absorption spectra.

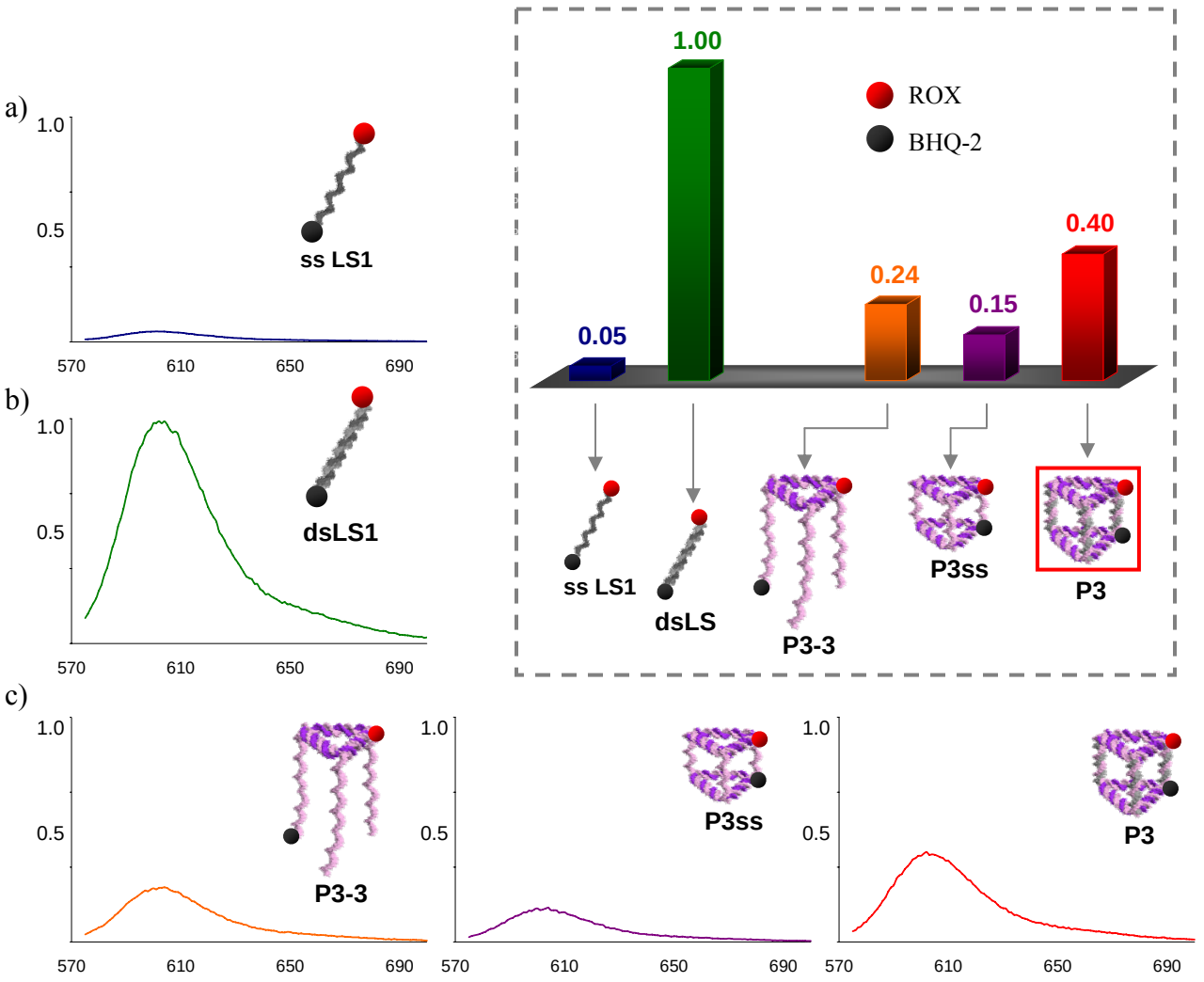

Figure S7. Normalized fluorescence measurements obtained from the (a) single-stranded and (b) double-stranded end-labeled fluorescence probe **LS1**. (c) FRET analysis of the intermediate assemblies in which a single unit of triangle **3** hybridized to three single-stranded linker strands (left), of two units of triangle **3** hybridized to three linker strands (center), and of fully double-stranded well-defined prism **P3** (right). A bar graph containing the relative intensity of each of these species, at 602 nm, summarizes these results (inset).

Table S3. Linker strands **LS 1-6** and rigidifying strand **RS1**.

	Sequence (5' → 3')
LS1	TGACATCACCACGACATCTCCACAAATCGG
LS2	TTGGTTGGCTACGACATCTCTGACCAATAA
LS3	GCTCATACTCACGACATCTCTTCAACCTAA
LS4	AAATCTGGCTACGACATCTCCAGCAAACCT
LS4	GACATCACCTACGACATCTCCAAGAGTTCC
LS6	TGGACGCCCGACGACATCTCTTCCTACCTT
RS1	GAGATGTCGT

Access to square **P4** (i.e. cube), pentameric **P5** and hexameric prism **P6** is conducted in a similar manner (3 X 10^{-10} moles of final assembly in 10µL TAEmg, 0ºC, 15 minutes). Scheme S4 outlines the building blocks used in generating each of these prisms, while Table S3 lists the sequences of the linker and rigidifying strands used to generate **P3-P6**. The quantitative assembly of **P4**, **P5** and **P6** is characterized using a 10% native polyacrylamide gel (Figure S8), and is confirmed following digestions with both MBN and ExoVII (Figure S9).

Scheme S4

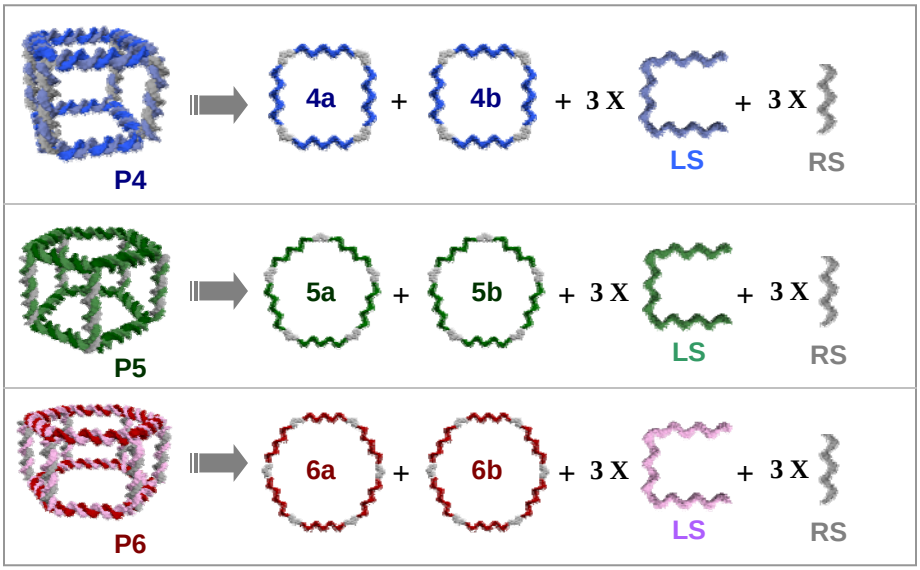

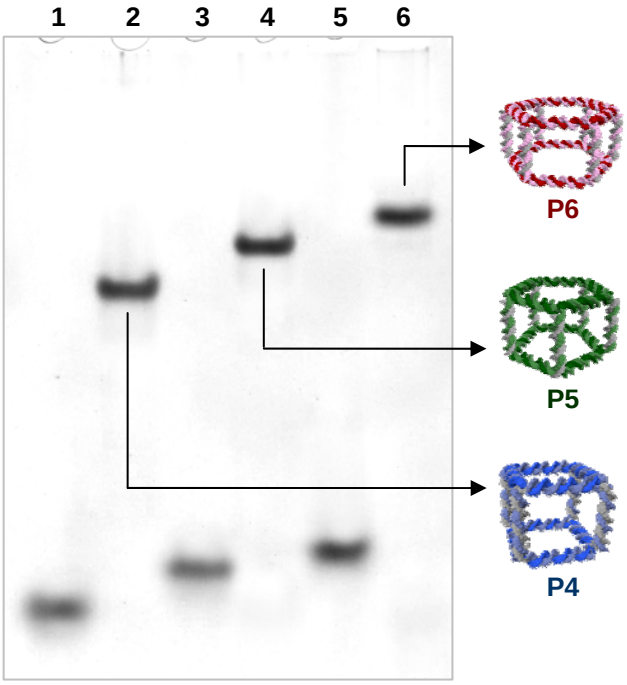

Figure S8. Cyclic DNA building blocks square **4** (lane 1), pentamer **5** (lane 3) and hexamer **6** (lane 5) are used to quantitatively generate square **P4** (lane 2), pentameric **P5** (lane 4) and hexameric prism **P6** (lane 6)**,** respectively.

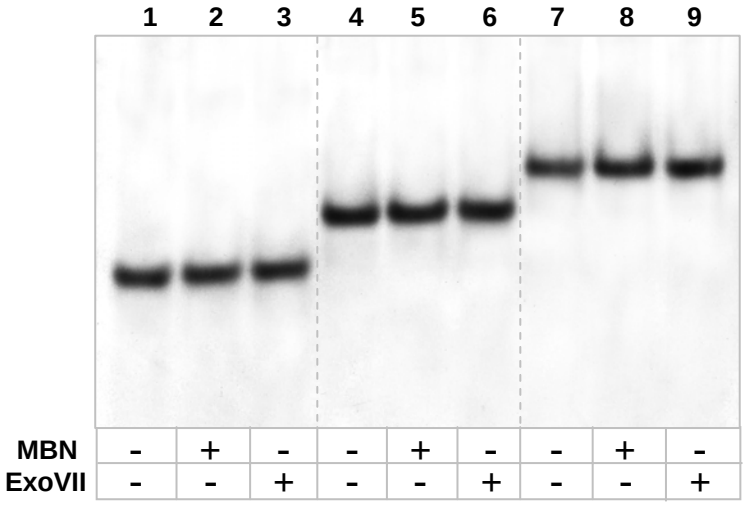

Figure S9. Square **P4** (lane 1), pentameric **P5** (lane 4) and hexameric prism **P6** (lane 7) were unaffected by enzymatic digestions with either MBN or ExoVII (lanes 2 and 3, lanes 5 and 6, and lanes 8 and 9, respectively).

V. Heteroprism HP and biprism BP

Self-assembly of heteroprism **HP** was conducted using one unit of triangle **3**, one unit of hexamer **6** and three linker strands of appropriate sequence, while access to biprism **BP** was conducted using two units of triangle **3**, one unit of hexamer **6** and six linker strands (Scheme S6). It is of interest to note that in the case of **HP**, the final assemblies were rigidified following addition of strands that are complementary to both the linker strands and the three remaining unhybridized positions on hexamer **6**. Table S4 contains the sequences of the linker strands and of the rigidifying strands used.

Scheme S5

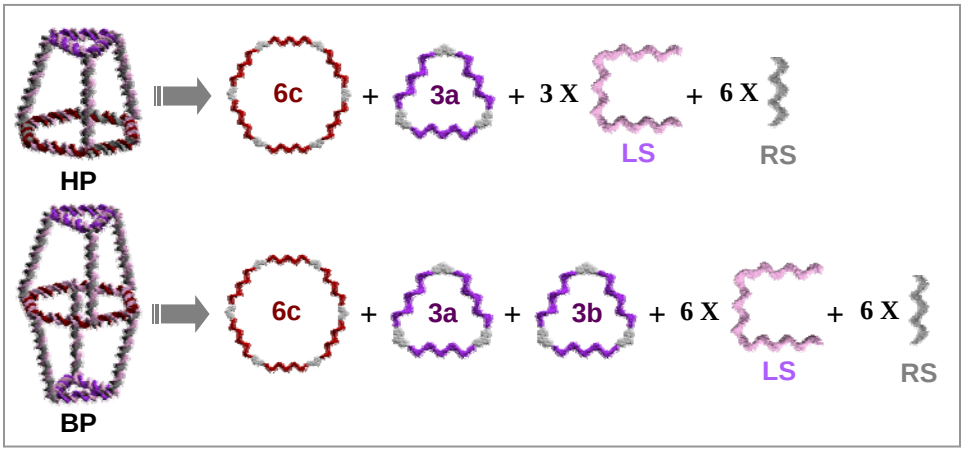

Self-assembly was conducted by mixing all building blocks in the correct molar ratio (3 X 10^{-10} moles of the final assembly), in 10 μL of TAEmg, and by incubating on ice for 15 minutes. Sequential analysis of the intermediates leading to, and including, heteroprism **HP** and biprism **BP** are performed using 10% native polyacrylamide gel electrophoresis (Figure 2, manuscript). In all cases, the assemblies proceed quantitatively.

Table S4. Sequences of linker and rigidifying strands used to generate **HP** and **BP**.

	Sequence (5' → 3')
6c	TTGACCAAGATAACACAGATAGACAGGTGACCTCCACACTC GACCCCTAACAATCGACCT
Tc	GTCAAAGGTC
LS7	TTCAACCTAAATGCCGATCGATAGCTAGCTATCTGTGTTA
LS8	TGACCAATAAATGCCGATCGATAGCTAGCTAGTGTGGAGG
LS9	CACAAATCGGATGCCGATCGATAGCTAGCTCAATCGACCT
LS10	TTGGTTGGCTATGCCGATCGATAGCTAGCTTCACCTGTCT
LS11	GCTCATACTCATGCCGATCGATAGCTAGCTTTAGGGGTCG
LS12	TGACATCACCATGCCGATCGATAGCTAGCTTCTTGGTCAA
RS2	AGCTAGCTATCGATCGGCAT
RS3	TCTTGGTCAA
RS4	TCACCTGTCT
RS5	TTAGGGGTCG

The connectivity of both heteroprism **HP** and biprism **BP** was also confirmed using enzymatic digestion assays with MBN and ExoVII. As seen in Figure S10, **HP** and **BP** were unaffected by digestions from either enzyme, and are thus fully double-stranded and cyclic in nature.

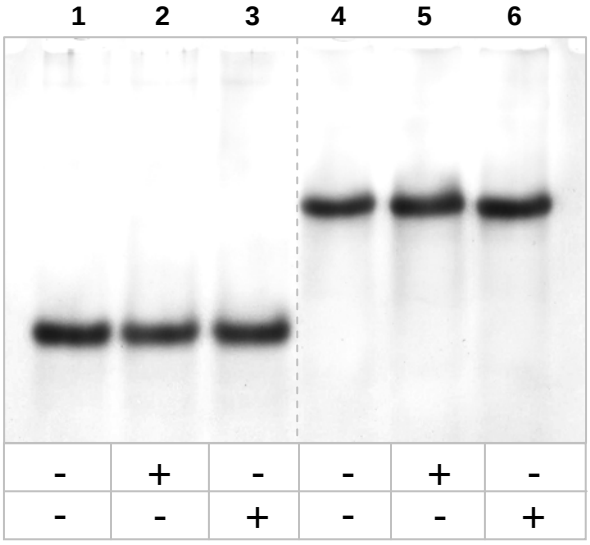

Figure S10. Both heteroprism **HP** (lane 1) and biprism **BP** (lane 4) were unaffected by enzymatic digestion with either MBN or ExoVII (lanes 2 and 3, and lanes 5 and 6, respectively).

FRET studies were conducted on biprism **BP** in order to monitor the addition of both triangular apices to the hexameric equatorial unit (Figure S11). Linker strands **LS7** and **LS10**, each end-labeled with the fluorophore and quencher ROX / BHQ-2, were used to probe hybridizations of hexamer **6b** to

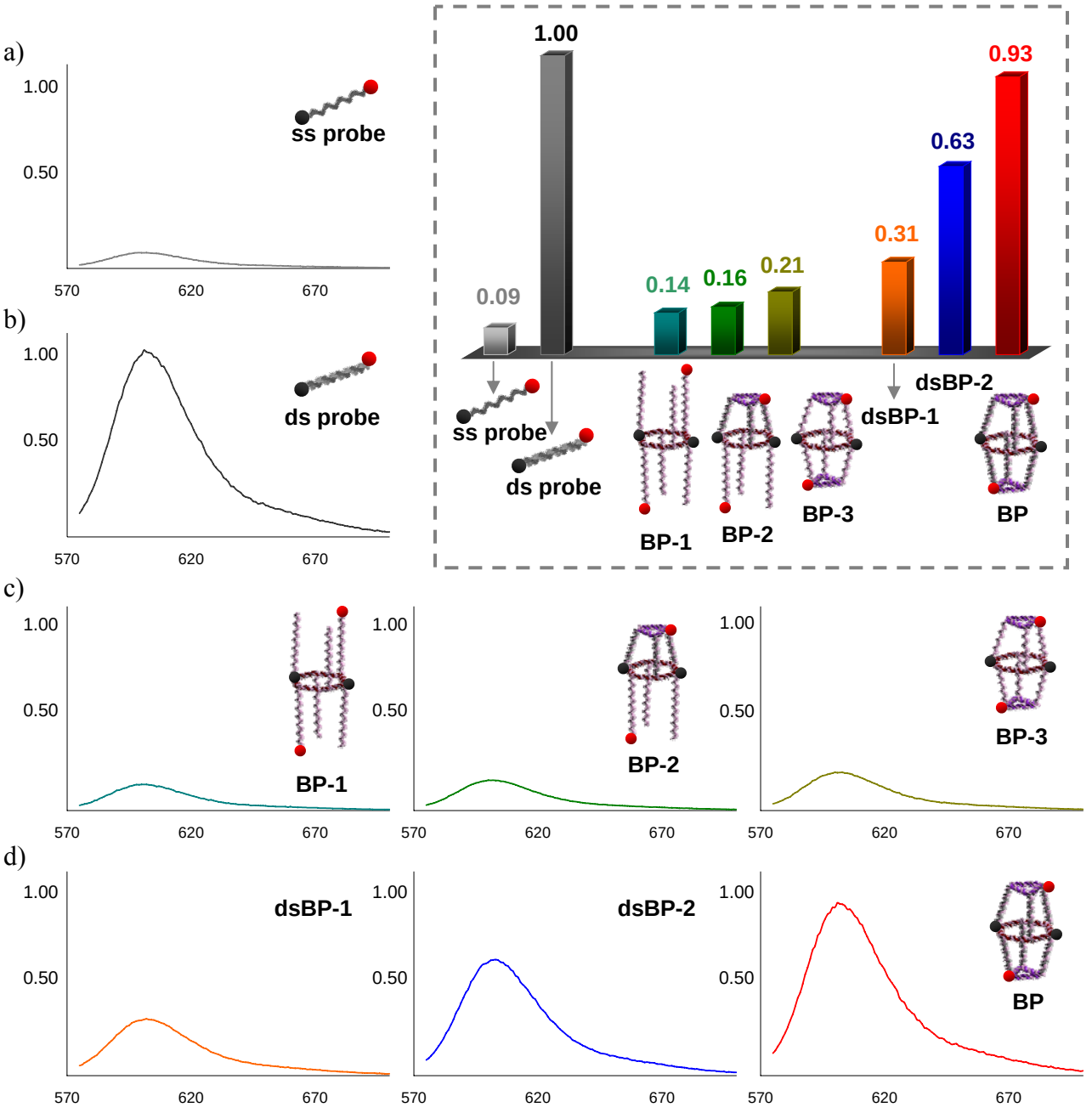

Figure S11. Normalized fluorescence measurements obtained from the (a) single-stranded and (b) double-stranded analogues of dually the end-labeled probe **LS7**. FRET studies on the (c) single-stranded and (b) double stranded intermediates leading to the generation of biprism **BP**. A bar graph containing the relative intensity of each of these species, at 602 nm, summarizes these results (see inset at the upper right corner).

triangle **3a** and triangle **3b**, respectively. In all cases, measurements were performed on 2 X 10^{-10} moles of the final capsule, in a total volume of 75 μL of TAEmg buffer and at 25ºC. The assembly intermediate **dsBP-1**, hexamer **6b** hybridized to six double strnaded linker strands **LS 1-6** (two of which are labeled with ROX / BHQ-2), emits at 31% the totally unquenched probe. Addition of the first triangular unit **3a** to generate **dsBP-2** results in an increase to 63%, while the addition of the second triangular unit **3b** to generate **BP** results in an even greater increase to 93%. These observations support the two-step clipping of two triangular units onto the two faces of cyclic hexamer **6** to generate biprism **BP**.

VI. Structural modulation between three predefined lengths of prism dynP

Triangular prism **dynP** capable of structural switching between three predefined lengths was constructed. **dynP** is assembled from two units of triangle **3a**, triangle **3b**, and from three linking strands that are each 40 bases long. This set of linking strands provides a 20 base single-stranded region that spans both ends of prism **dynP**. It is this partially single-stranded synthetic intermediate that is then used to generate the three well-defined fully double-stranded triangular prisms of different lengths **dynP10**, **dynP14** and **dynP20**. As seen in Scheme S6, the use of rigidifying strands **9** that are fully complementary result in fully extended 20 base long triangular prisms **dyn20**, the incorporation of a 6 base internal loop using rigidifying strands **8** that are 24 bases long generates 14 base long triangular prisms **dynP14**, while the incorporation of a 10 base internal loop using rigidifying strands **7** that are 20 bases long generates **dynP10** with a length of 10 bases. The last 10 bases of each rigidifying strand is in fact a 10 base overhang that allows for the strands' addressable removal upon its hybridization to fully complementary eraser strands (**12**, **11** and **10**, respectively). This is done in order to allow for real-time cycling between the three defined dimensions of prism **dynP**. The sequences of the linker and rigidifying strands used is summarized in TableS5.

Scheme S6

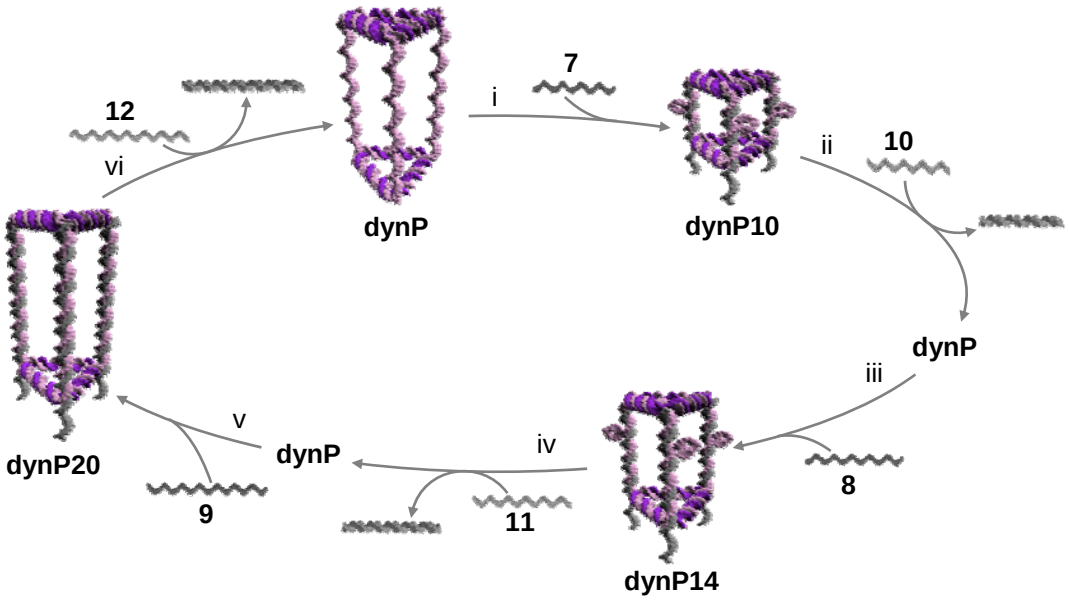

(i) Well-defined triangular prism **dynP10** is generated from **dynP** following the addition of RS which incorporate 10 base internal loops. (ii) Eraser strands fully complementary to the respective RS are used to regenerate **dynP10** from **dynP10**. (iii) Addition of rigidifying strands that incorporate a 6 base internal loop result in well-defined assembly of triangular prism **dynP14**. (iv) This prism is dis-assembled to regenerate **dynP** following the addition of fully complementary eraser strands. (v) Fully complementary RS result in prism **dynP20**, with a length of 20 bases. (vi) The cycle is completed by the addition of eraser strands which are fully complementary to the RS used in **dynP20**.

Table S5. Sequences of the linker strands **LS**, rigidifying strands **RS**, and their respective complements **RSerase**, used to generate and cycle between the different states of **dynP**.

	Sequence (5' → 3')
LS13	TGACATCACCATGCCGATCGATAGCTAGCTCACAAATCGG
LS14	TTGGTTGGCTATGCCGATCGATAGCTAGCTTGACCAATAA
LS15	GCTCATACTCATGCCGATCGATAGCTAGCTTTCAACCTAA
RS6 (20mer)	ATGCCGATCGATAGCTAGCTACGCATCTC
RS6erase	GAGATGTCGTAGCTAGCTATCGATCGGCAT
RS7 (24mer)	ATGCCGAGCTAGCTACGACATCTC
RS7erase	GAGATGTCGTAGCTAGCTCGGCAT
RS8 (30mer)	ATGCCTAGCTACGACATCTC
RS8erase	GAGATGTCGTAGCTAGGCAT

Self-assembly of the single-stranded analogue of prism **dynP** was conducted by combining the respective building blocks in the correct molar ratio (5 X 10^{-10} moles of final assembly), in 10 μL of TAEmg buffer, and by incubating at 0ºC for 15 minutes. Gel electrophoresis analysis of this initial intermediate revealed the quantitative generation of a single product (Figure 3, manuscript), while FRET measurements using ROX / BHQ-2 end-labeled linker strand **LS13** showed an emission peak with FRET efficiency of 14% (Figure S12). A full structural modulation cycle using **dynP** is conducted as follows:

1) Addition of 20mer rigidifying strands to **dynP** generates well-defined triangular prism **dynP10** with an experimentally calculated length of 5.2 nm (Figure 3b manuscript, Figure S12b).
2) Addition of 20mer eraser strands to the assembly of **dynP10** regenerates the partially single-stranded intermediate **dynP** (Figure 3b manuscript, Figure S12c).
3) Addition of 24mer rigidifying strands to the previously generated **dynP** results in triangular prism **dynP14**, with an experimentally calculated length of 6.9 nm (Figure 3b manuscript, Figure S12d).
4) Addition of 24mer eraser strands to the previous assembly of **dynP14** regenerates the partially single-stranded intermediate **dynP** (Figure 3b manuscript, Figure S12e).
5) Addition of 30mer rigidifying strands to the previously generated **dynP** results in prism **dynP20**, with an experimentally calculated length of 8.9 nm (Figure 3b manuscript, Figure S12f).
6) Finally, the addition of 30mer eraser strands to **dynP20** regenerates the initially constructed intermediate **dynP**, and thus completes the structural cycle (Figure 3b manuscript, Figure S12g).

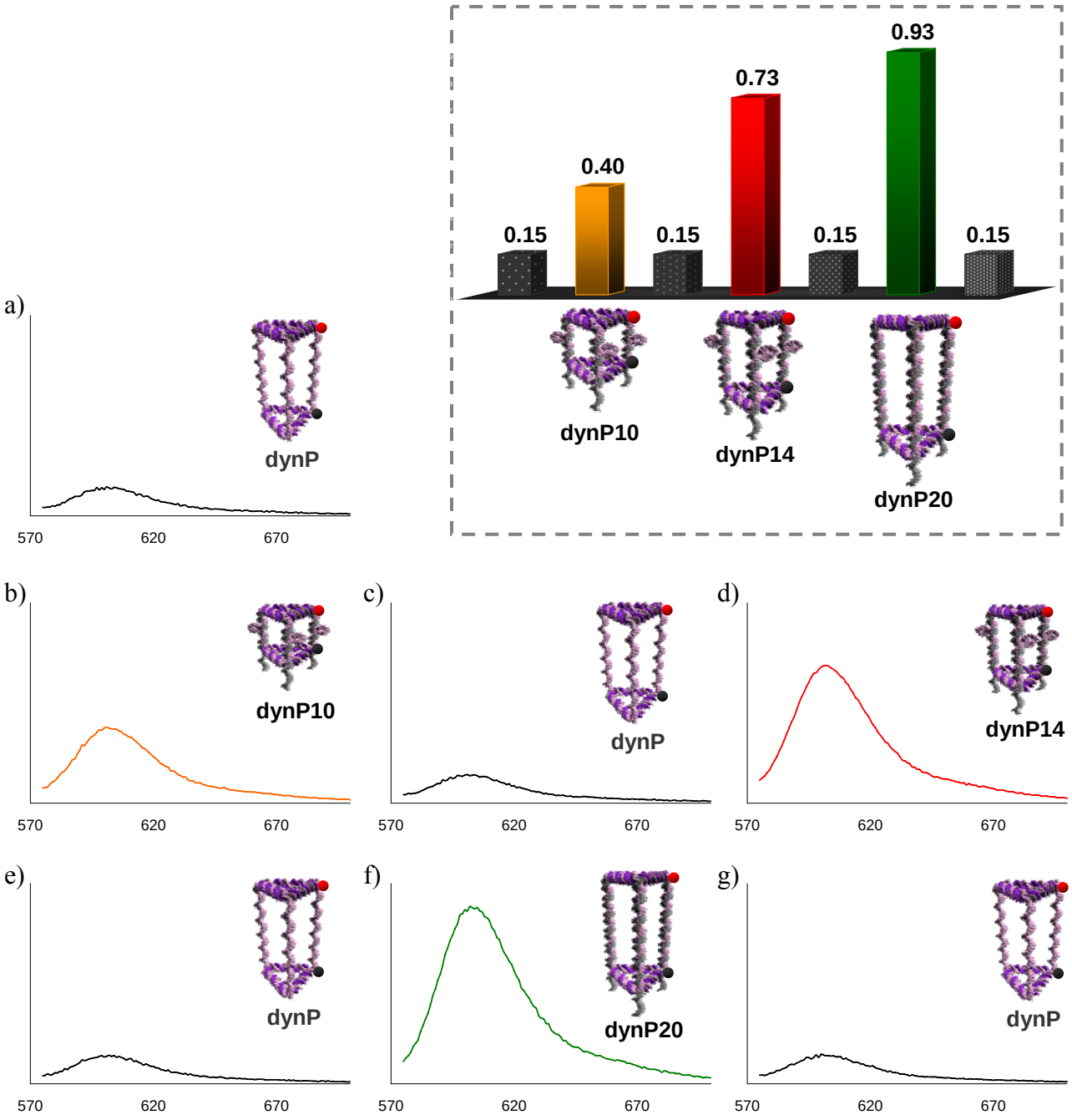

Figure S12. FRET analysis of the intermediates within a complete structural cycle for triangular prism **dynP** (see inset for summary). The single stranded analogue is used to generated prism **dynP10** with a length of 10 bases. The rigidifying strands within this assembly are then removed to regenerate the single-stranded analogue **dynP**, and are replaced with a set that constructs a 14 base long prism **dynP14**. This prism is similarly turned into **dynP**, and is then used to generated the 20 base long prim **dynP20**. The first member of this cycle dynP is finally regenerated by removal of the set of rigidifying strands.

It is of interest to note that a difference in electrophoretic mobility between the 10, 14 and 20 base long prisms is expected. And that it was not possible to run the samples in the gel in Figure 3b (manuscript) any longer without over-running the lower bands corresponding to the double stranded 20mer, 24mer and 30mers past the front line of the gel. Therefore, a separate experiment was conducted in which the gel was run longer (120 V, 10 mA, 17 hours, 0ºC) in order to allow for a truly representative analysis of the differences in mobility between the three prismic species. As expected, **dynP14** is slightly retarded in mobility when compared to **dynP10**, and **dynP20** is retarded even more so (Figure S13).

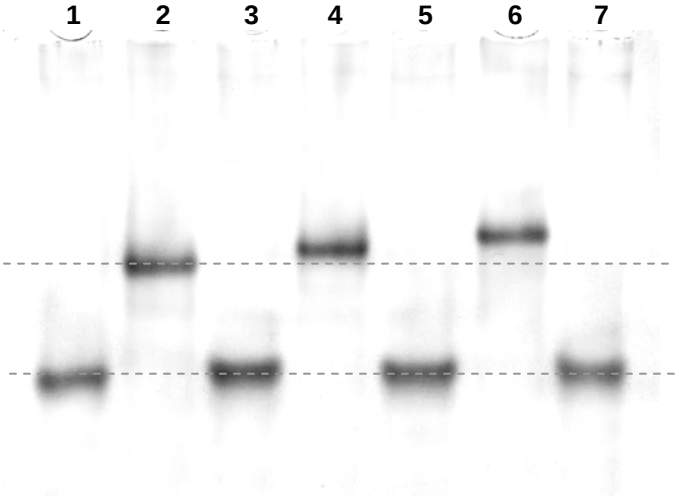

Figure S13. 10% native polyacrylamide gel of the three states of the structurally dynamic triangular prism **dynP3**. Lanes 1, 3, 5 and 7 contain the single-stranded intermediates, while lanes 2, 4 and 6 contain prism **dynP** with lengths corresponding to 10, 14 and 20 bases.

VII. References

S1 Reference 4 in manuscript.

S2 Distler, A. M.; Allison, J. *Anal. Chem.* **2001**, *73,* 5000-5003.

S3 Carriero, S.; Damha, M. J.; *Org. Lett.* **2003**, 5(3), 273-276.

S4 (a) Kroeker, W. D.; Kowalski, D.; Laskowski, M. Sr. *Biochemistry* **1976**, *15,* 4463-4467. (b) Johnson, P. H.; & Laskowski M. Sr. *J. Biol. Chem.* **1970**, *245,* 891-898.

S5 Lackowitz, J. R. in *Principles of Fluorescence Spectrosopy*; Kluwer/Plenum Publishers: New York, 1999.